Palaeogeography, Palaeoclimatology, Palaeoecology
April 2022, Volume 592, Pages 110898 (10p.)
https://doi.org/10.1016/j.palaeo.2022.110898
https://archimer.ifremer.fr/doc/00753/86476/

Production of short-chain n-fatty acids in coral reefs in the southern South China Sea since the Late Miocene

Zhu Xiaowei [1, 2], Li Gang [1, 2], Tian Yuhang [1, 2], Xu Weihai [1, 2, *], Miao Li [1, 2], Liu Jianguo [1, 2], Luo Yun [1, 2], Cheng Jun [1, 2, 3], Zhang Lulu [1, 2, 3], Wang Shuhong [1, 2], Yan Wen [1, 2, 3, *]

[1] Key Laboratory of Ocean and Marginal Sea Geology, South China Sea Institute of Oceanology, Innovation Academy of South China Sea Ecology and Environmental Engineering, Chinese Academy of Sciences, Guangzhou 510301, China
[2] Southern Marine Science and Engineering Guangdong Laboratory (Guangzhou), Guangzhou 511458, China
[3] University of Chinese Academy of Sciences, Beijing 100049, China

* Corresponding authors : Weihai Xu, email address : whxu@scsio.ac.cn ; Wen Yan, email address : wyan@scsio.ac.cn

Abstract :

The monsoon system modulates surface production in the South China Sea (SCS). The winter monsoon has long been recognized as the primary factor regulating surface production in the northern SCS; however, the role of monsoon remains in debate in the southern SCS. Here, we present a long record of short-chain n-fatty acids (n-FAs) in reefal carbonates from one deep well (NK1) on an isolated coral atoll (Meiji) in order to provide new insights into the change of surface production in the southern SCS since the Late Miocene (ca. 10.5 Ma). Short-chain n-FAs indicative of total marine organic matter input are rather feasible to reflect the total production associated with mixotrophic reef-building corals that feed on various marine biotas (i.e., phytoplankton, zooplankton and bacteria). By ruling out the significant influence of diagenetic and degradation processes, short-chain n-FAs can be further applied to reconstruct paleo-production in Well NK1 coral reefs. The temporal distribution of short-chain n-FAs changes similarly with many other independent paleo-production records (i.e., Ln(Ba/Ti) and opal) in Well NK1 and adjacent ODP Site 1143, demonstrating the close coupling between coral reef production and surface water production. This occurs through the common factor of nutrients in modulating production of symbiotic autotrophic coralgae and asymbiotic phytoplankton and/or the large heterotrophic dependence of corals on phytoplankton-governed food webs in surface waters. Short-chain n-FAs inferred surface production displays a progressively decreased trend from the Late Miocene to Pliocene (ca. 10.5–2.6 Ma) followed by a substantial increase since the Pleistocene on million-year timescales, which follows the variation of terrigenous supply to the coral atoll and responds almost inversely to the sea-level change. Accordingly, we propose that long-term paleo-production in the southern SCS was associated with terrestrial nutrient input which was controlled by relative sea-level change since the Late Miocene. This study highlights the feasibility of short-chain n-FAs as appropriate production recorders in shallow-water coral reefs which are widespread in tropical-subtropical oceans, providing valuable perspectives on long-term paleo-production evolution in surface waters.

Highlights

► A long coral reef well (NK1) in the southern SCS was studied. ► OM-poor coral reef carbonates were decalcified and extracted for biomarkers. ► Short-chain *n*-FAs reflect paleo-productivity in coral reefs since the Late Miocene. ► Long-term productivity was governed by terrestrial nutrient related to sea level.

Keywords : Words: coral reef carbonates, lipid biomarkers, production, southern South China Sea, Late Miocene

1. Introduction

Phytoplankton, accounting for almost half of the biosphere's primary production (Field et al., 1998), is fundamental to a vast majority of consumers in marine food webs (Chassot et al., 2010). In addition to ecological function, phytoplankton plays a crucial role in regulating Earth's climate through the biological pump that sequestrates atmospheric CO_2 into the ocean interior by photosynthesis (Falkowski et al., 1998;

Sigman and Boyle, 2000; Falkowski, 2012). The instantaneous rate of phytoplankton production is critically limited by light availability in the euphotic zone in the contemporary ocean (Field et al., 1998), but as long as nutrients brought into the euphotic zone are eventually consumed, the total production is largely dependent on nutrient availability linked to oceanic and atmospheric dynamics (Falkowski et al., 1998). Therefore, the change in nutrient budgets delivered to the marine euphotic zone will result in significant feedbacks on global biogeochemical cycles and climate systems by regulating phytoplankton production. Though featured by the distinct low production in surface waters, the oligotrophic low-latitude Pacific-Indian-Atlantic Oceans (Falkowski et al., 1998; Field et al., 1998) still play an important role for the global oceanic biological pump due to a vast proportion in the euphotic zone.

As the largest marginal sea in the western Pacific, the South China Sea (SCS) contains a broad eutrophic continental shelf and a large oligotrophic deep basin. The seasonally reversing monsoon is generally proposed as the primary driver for surface production in offshore waters by modulating nutrients from below through mixing and upwelling (Liu et al., 2002; Ning et al., 2004; Tang et al., 2004, 2006; Zhang et al., 2016). The paleo-production records in the northern SCS are generally attributed to the winter monsoon variability and intensity, showing elevated production during glacial mixing/upwelling periods (He et al., 2013; Zhang et al., 2016; Han et al., 2019; Zhu et al., 2020). However, the importance of monsoon on surface production in the southern SCS remains a matter of debate. For example, a phytoplankton-biomarker study on core MD05-2901 reveals only an insignificant change of total phytoplankton production during glacial-interglacial cycles (Li et al., 2015). In contrast, studies on marine organic carbon in core 17962 (Jia et al., 2002) and biomarkers of ammonia oxidizing *Thaumarchaea* in core MD05-2897 (Dong et al., 2019) point to enhanced

production during glacial periods, whereas most other studies on biogenic elements (i.e., Ba), siliceous (i.e., opal, diatom and radiolarian) and foraminifera assemblages observe higher production associated with intensified summertime upwelling in interglacial times (Jian et al., 2001; Wang and Abelmann, 2002; Wang and Li, 2003; Li et al., 2018). These inconsistencies indicate that the controlling factors on paleo-production in the southern SCS seem to be more heterogeneous as proposed so far.

Shallow-water coral reefs, widespread in tropical-subtropical oceans including the SCS, are formed by symbiotic reef-building corals that inhabit the euphotic zone (Yu, 2012). As mixotrophic organisms, reef-building corals obtain nutrients from autotrophic photosynthesis by endosymbiotic coralline algae and heterotrophic predation on external various food resources (i.e., phytoplankton, zooplankton and bacteria) in surface waters (Wood, 1993, 1995; Anthony and Fabricius, 2000; Houlbrèque and Ferrier-Pagès, 2009). Under the condition of autotrophy, coral autotrophic production by symbiotic algae (i.e., dinoflagellats) correlates in concert with surface production by asymbiotic phytoplankton (i.e., diatoms) due to the common factor of nutrients in the euphotic zone (e.g., He et al., 2013; Li et al., 2015; Zhu et al., 2021). In the case of heterotrophy, coral heterotrophic production also relates in coupling to surface production due to the large dependence of corals feeding on asymbiotic phytoplankton (and phytoplankton-governed secondary consumers, i.e., zooplankton and bacteria) in surface waters (Wood, 1993, 1995). The close coupling between the production of mixotrophic reef-building corals and surface phytoplankton production may thus allow shallow-water coral reefs to provide unique insights into surface production in the past.

Lipid biomarkers, which are primarily derived from once-living organisms and

are generally resistant to weathering, biodegradation, evaporation and other processes (Peters et al., 2005), have high potential to give unique clues for paleo-production in coral reefs. As the major component (up to 73%) in coral total lipids (Treignier et al., 2008; Tolosa et al., 2011), fatty acids (FAs) are composed mainly of short-chain *n*-FAs in many corals (e.g., Imbs and Yakovleva, 2012; Kneeland et al., 2013; Radice et al., 2019; Rocker et al., 2019). The dominance of short-chain *n*-FAs occurs also in marine geological archives (i.e., sediments) likely due to their ubiquity in various marine biotas, including phytoplankton, zooplankton and bacteria (Dalsgaard et al., 2003; Volkman, 2006). In view of this character, short-chain *n*-FAs are widely applied to indicate total marine organic matter (OM) input (Mudge and Norris, 1997; Gogou and Stephanou, 2004; Treignier et al., 2006; Hu et al., 2009; Strong et al., 2012, 2013; Zhu et al., 2014, 2021; Guo et al., 2019). Thus, given the incorporation of various marine organisms into reef-building corals through autotrophic and heterotrophic pathways (Anthony and Fabricius, 2000; Houlbrèque and Ferrier-Pagès, 2009), short-chain *n*-FAs are likely feasible to document the production in mixotrophic reef-building corals and their reef builders. Here, lipid biomarker analysis is applied to Well NK1 coral reefs, aiming to: (1) elucidate the ability of short-chain *n*-FAs for reconstruction of paleo-production in coral reefs and in surface waters, and (2) revisit potential factors regulating long-term production evolution in the southern SCS since the Late Miocene (ca. 10.5 Ma).

2. Materials and Methods

2.1 Study area and samples

The SCS surface hydrology responds actively to the monsoon system, showing a basin-wide cyclonic circulation in winter (or winter monsoon) and a large-scale

anticyclonic circulation in summer (or summer monsoon) (Fig. 1B) (Fang et al., 1998). The monsoon plays a vital role in spatiotemporal variations of surface production in the SCS and high production is present in seasonal upwelling regions, such as the summer monsoon-induced Vietnam Upwelling (Fig. 1B) (Liu et al., 2002; Ning et al., 2004; Tang et al., 2004, 2006). In addition to upwelling-induced high nutrients, terrestrial riverine nutrient influx from the Mekong River plays an important role in fertilizing high production in the coastal Vietnam (Liu et al., 2002; Ning et al., 2004; Tang et al., 2004, 2006). These marine upwelling and terrestrial riverine associated nutrients can also exert a large-spatial influence on surface water production from coastal Vietnam to offshore southern SCS due to oceanic circulation (Fig. 1B) (Liu et al., 2002; Tang et al., 2004, 2006).

Well NK1 (2020.2 m in length) was drilled on the Meiji Atoll, which belongs to the Nansha Islands in the southern SCS (Fig. 1). The lower parts (997.7–2020.2 m) of Well NK1 are composed of basic rocks, and coral reef carbonates comprise the upper intervals (2.6–997.7 m) with a recovery up to 92%. This study focuses on a proportion of (upper ca. 500 m) carbonate sequences, corresponding to a history since the Late Miocene (ca. 10.5 Ma) based on well-established chronological framework as reported in detail in previous studies (Luo et al., 2021, 2022; Yi et al., 2021; Li et al., accepted). The detailed mineral, isotopic and elementary date of Well NK1 can be found in Guo et al. (2021) and Luo et al. (2021, 2022).

2.2 Pre-cleaning, lipid extraction and analysis of lipid biomarkers

As lipid biomarker inventory recovered from OM-poor carbonates (i.e., stalagmites) is susceptible to contamination, the pre-cleaning procedures proposed previously for stalagmites (Blyth et al., 2006) were also performed on our coral reef

carbonate samples, as well as glassware, reagents and consumables used in this study. Carbonate samples with visible high compaction were preferentially selected for lipid biomarker analysis because of their low porosity, which diminishes contamination and microbial degradation after lithification (Heindel et al., 2010). Subsequently, carbonate fragments containing external surfaces were cut to keep the central pillars with a diamond cutter bar (Supplementary Fig. S1A). The fresh pillar samples were then cleaned with deionized water, ethyl alcohol and dichloromethane (DCM) successively in an ultrasonic bath (Supplementary Fig. S1B), afterwards they were oven-dried and powdered with an agate mortar and pestle.

Lipids are usually present in very low concentration in carbonates and are partly trapped within the crystals so that conventional solvent extraction method (i.e., ultrasonic and soxhlet) only recovers lipid biomarkers from free OM pool (Blyth et al., 2006). Therefore, an acid digestion method proposed initially for stalagmites (Blyth et al., 2006; Wang et al., 2012) was used to extract most lipid biomarker yields from Well NK1 coral reef carbonates by releasing carbonate-trapped and chemically-bound OM. A similar decalcification and extraction protocol has been applied to recover lipid biomarkers from reefal microbialites (Heindel et al., 2010, 2012; Braga et al., 2019). Briefly, aliquot powdered carbonates (10 g) were digested in pre-cleaned HCl (3 M) and then boiled under reflux for 3 h (Supplementary Fig. S1C), followed by the extraction with pre-redistilled DCM in a separating funnel (Supplementary Fig. S1D).

Further, one sample (at 108.39 m) was measured for a comparison between the Total Lipid Extract (TLE; Supplementary Fig. S2A) from one aliquot (10 g) and individual lipid (i.e., alcohol and FA; Supplementary Figs. S2B–C) classes separated from the TLE of the four aliquots (10 g × 4). A method similar to that of Zhu et al. (2014) was used for lipid class separation. Briefly, following saponification with

KOH/MeOH (1 M), the neutral fractions were extracted with *n*-hexane and the residuals were treated with acidification to obtain the FA fraction. The neutral lipids were purified using silica gel chromatography by elution with *n*-hexane and MeOH to get alkanes and alcohols, respectively. The TLE (from one aliquot) and separated alcohol and FA fractions (from four aliquots) were converted to trimethylsilyl derivatives with bis(trimethylsilyl)trifluoroacetamide (BSTFA) at 60 °C for 2 h prior to gas chromatography–mass spectrometry (GC–MS) analyses. The separation of different lipid classes did not yield more kinds of biomarkers (Supplementary Fig. S2), implying that almost all the biomarkers in the TLE are well above the detection limit. Therefore, for simplicity, the TLE without further separation was analyzed to show a general composition and distribution of lipid biomarkers in Well NK1 in this study.

GC–MS analysis was performed at the State Key Laboratory of Organic Geochemistry, Guangzhou Institute of Geochemistry, Chinese Academy of Sciences, with a Thermo Scientific Trace gas chromatograph coupled to a Thermo Scientific DSQ II mass spectrometer. Separation was achieved with a 60 m × 0.32 mm i.d. fused silica column (J & W DB-5) coated with a 0.25 μm film thickness. The oven temperature was programmed from 80 °C (held 2 min) to 160 °C at 6 °C/min, and then to 270 °C at 3 °C/min, and at last to 310 °C (held 30 min) at 8 °C/min. Helium was used as the carrier gas at 1.1 ml/min. The ion source was operated in the electron ionization (EI) mode at 70 eV, and a full scan mode in a range of *m/z* 50–750 was applied.

3. Results

3.1 Lipid biomarker compositions

A great variety of FAs are identified in Well NK1 coral reef carbonate samples (Supplementary Fig. S2A), with *n*-FAs being the predominant constituents (ranged

0.4–18.2 μg/g and avearged 7.1 ± 5.0 μg/g bulk carbonate) followed by second abundant unsaturated FAs (ranged 0.0–9.3 μg/g and avearged 2.5 ± 2.4 μg/g) and minimum *br*-FAs (ranged 0.0–1.4 μg/g and avearged 0.2 ± 0.2 μg/g) (Fig. 2A). The *n*-FAs are composed of short-chain homologs (C_{12}–C_{24}) dominated by C_{16} and C_{18} (ranged 0.2–8.3 μg/g and 0.2–5.8 μg/g, and accounted for averaged 54.1% ± 8.7% and 35.1% ± 9.4% in total *n*-FAs, respectively) (Fig. 2B). The *n*-$C_{22:1}$ FAs (the sum of *n*-$C_{22:1\omega9}$ and *n*-$C_{22:1\omega7}$) are the most abundant components (ranged 0.0–8.2 μg/g and avearged 2.1 ± 2.1 μg/g) in unsaturated FA class, accounting for averaged 78.7% ± 22.2% (Fig. 2C). The *i*-C_{16} is slightly more abundant, accounting for averaged 29.8% ± 8.0% in total *br*-FAs, followed by relatively equivalent *a*-C_{15} (22.1% ± 14.6%), *a*-C_{17} (17.6% ± 24.9%), *i*-C_{17} (17.3% ± 15.5%), *i*-C_{15} (16.6% ± 6.5%) and *i*-C_{14} (16.4% ± 9.4%) (Fig. 2D).

In alcohol fraction, only *n*-alcohols are detected (Supplementary Figs. S2A–B), which have significantly lower abundances (ranged 0.1–2.0 μg/g and averaged 0.5 ± 0.3 μg/g) than *n*-FA counterparts (Fig. 2A). The *n*-alcohols also consist of short-chain homologs (C_{14}–C_{20}), but are dominated solely by C_{18} (ranged 0.0–1.8 μg/g and accounted for avearged 87.3% ± 8.3% in total *n*-alcohols) (Fig. 2E).

As the major components in alkane class, *n*-alkanes are dominated by short-chain homologs (accounted for averaged 71.0% ± 13.8% in total *n*-alkanes) with rather low contents as compared to FAs and alcohols in most samples (Supplementary Fig. S2A). The alkane fraction is not further discussed in this study due to the absence of diagnostic biomarkers, as suggested previously (Heindel et al., 2010, 2012; Braga et al., 2019), but the pristine/phytane (Pr/Ph) ratio (ranged 0.14–0.83) is used in the following discussion.

3.2 Distribution of lipid biomarker in Well NK1

Contents of *n*-$C_{14–18}$ FAs, *n*-$C_{22:1}$ FAs, *br*-FAs and *n*-$C_{14–18}$ alcohols exhibit good positive correlations with each other (Supplementary Table S1), thereby allowing for *n*-$C_{14–18}$ FAs to provide a general view of the biomarker distribution in upper ca. 500 m of Well NK1. The distribution of *n*-$C_{14–18}$ FAs can be divided into three intervals (Fig. 3): (1) relatively high contents (ranged 2.2–10.7 μg/g and avearged 4.6 ± 2.2 μg/g) with frequent oscillations at ca. 300–500 m intervals, (2) substantially lower abundances (ranged 0.4–5.4 μg/g and avearged 1.9 ± 1.4 μg/g) without significant change at ca. 120–300 m intervals, and (3) comparatively higher concentrations (ranged 1.2–14.7 μg/g and avearged 9.0 ± 4.0 μg/g) oscillated with varying degrees and large amplitudes and peaked at ca. 45–60 m and 95–115 m in upper ca. 120 m intervals.

4. Discussion

4.1 The feasibility of n-$C_{14–18}$ FAs for production of reef-building corals in Well NK1

The *n*-$C_{14–18}$ FAs (and *n*-alcohols) are generally used to reflect total marine OM input, including phytoplankton, zooplankton and bacteria (Mudge and Norris, 1997; Gogou and Stephanou, 2004; Treignier et al., 2006; Hu et al., 2009; Strong et al., 2012, 2013; Zhu et al., 2014, 2021; Guo et al., 2019); whereas *n*-$C_{22:1}$ FAs and *br*-FAs are usually specified to inputs of zooplankton and bacteria, respectively (Dalsgaard et al., 2003; Volkman, 2006). The abundant presence of these biomarkers in Well NK1 coral reefs (Fig. 2) likely indicates the incorporation of various marine biotas (and their lipids) into reef-building corals to support their growth and development through autotrophic and heterotrophic pathways. This is consistent with the predominance of modern *Porites* in the Meiji Atoll (Zhao et al., 2013) and the wide occurrence of

Porites corallites in Well NK1 (Luo et al., 2021; Zhao et al., 2021), as trophic strategies of stress-tolerant massive *Porites* are highly variable that can switch plastically between autotrophy and heterotrophy (Grottoli et al., 2006; Xu et al., 2020). Therefore, *n*-$C_{14–18}$ FAs, which are likely produced by external various food resources in surface waters before serving as dietary inputs for heterotrophic corals and/or produced in vivo by coral-associated autotrophic symbionts, are rationally feasible to reflect the total production of mixotrophic reef-building corals in Well NK1.

We notice the good positive correlations among *n*-$C_{14–18}$ FAs (and alcohols), zooplankton-derived *n*-$C_{22:1}$ FAs and bacteria-derived *br*-FAs in Well NK1 (Supplementary Table S1). Similar scenarios have also been documented in three shallow-water cores (water depths <35 m) in the northern SCS, showing strong correlations of phytoplankton-sterols with zooplankton-produced *n*-$C_{20:1}$ alcohols and *n*-$C_{14–18}$ alcohols (Zhu et al., 2021). These occurrences may reflect the close coupling among different groups of marine biotas (i.e., phytoplankton, zooplankton and bacteria) through food chains and their coupled contribution to the production of *n*-$C_{14–18}$ FAs and alcohols in the euphotic shallow-water zone.

4.2 Evaluation on the reliability of n-$C_{14–18}$ FAs as production recorders in coral reefs

As explained above, *n*-$C_{14–18}$ FAs indicative of total marine OM input are rather suitable to register total production associated with mixotrophic reef-building corals that feed on various marine organisms. However, before applying *n*-$C_{14–18}$ FAs as effective recorders of paleo-production in Well NK1 coral reefs, their suitability as such an approach should be examined. This is because *n*-$C_{14–18}$ FAs in reefal deposits may have undergone some alteration due to diagenetic and degradation processes, which can confound their implications for initial biotic precursors and related

environmental conditions. Here, the potential degradation loss of *n*-$C_{14–18}$ FAs in the euphotic shallow-water zone, where reef-building corals inhabit, is not considered, as the degradation of biomarkers has been found insignificant even in deep-sea water column (Prahl et al., 2000; Wakeham et al., 2002; Hernández-Sánchez et al., 2014). Therefore, in the following, we focus mainly on the potential influence of diagenetic alteration and degradation loss during burial in reefal carbonate deposits.

The diagenetic alteration mainly involved meteoric diagenesis under subaerial conditions and dolomitization forming in marine phreatic environments (Guo et al., 2021; Luo et al., 2021, 2022). Intensive meteoric diagenesis occurred mainly at ca. 20–120 m intervals and several limestone interlays at depths of ca. 440–500 m have experienced meteoric diagenesis (Fig. 3D) (Guo et al., 2021; Luo et al., 2021, 2022). The limestones forming in meteoric diagenetic environments are also accompanied by the pronounced negative signatures of $\delta^{13}C$ and $\delta^{18}O$ (Figs. 3B–C) and high contents of low-Mg calcite (Fig. 3D) (Guo et al., 2021; Luo et al., 2021, 2022). These isotopic and mineral characterizations have also been cited as the compelling evidence for the presence of extensive meteoric diagenesis on coral reefs of XC1 (Liu et al., 1997), ZK1 (Wang et al., 2018), and XK1 (Liu et al., 2019) in the Xisha Islands in the northern SCS. Therefore, the potential influence of carbonate diagenesis on *n*-$C_{14–18}$ FAs can be elucidated based on their correlation analyses with diagenetic proxy records of isotopes and minerals. As illustrated in Figs. 4A–B, contents of *n*-$C_{14–18}$ FAs display relatively strong negative correlations with values of $\delta^{13}C$ and $\delta^{18}O$, indicating the accelerated accumulation of *n*-$C_{14–18}$ FAs in correspondence to intense meteoric diagenesis. This occurrence should be attributed to the high terrigenous nutrient loading that fertilized the production in surface waters and in coral reefs due to reduced sea levels, as explained below. However, the comparatively high resistance

of lipid biomarkers in coral reef carbonates to post-depositional diagenesis should also be responsible for the coupling between abundant *n*-$C_{14–18}$ FAs and extensive meteoric diagenesis.

The high degradation of lipid biomarkers occurs usually under aerobic conditions (Hoefs et al., 2002; Sinninghe Damsté et al., 2002; Versteegh et al., 2010). Accordingly, the potential influence of degradation on *n*-$C_{14–18}$ FAs can be evaluated in the context of paleo-redox conditions. Shao et al. (2017a) proposed a simple redox framework of coral reefs in relation to sea-level changes, suggesting more reducing (marine) conditions during sea-level high stands and more oxidizing (subaerial) conditions with declined sea levels. Accordingly, the extensive subaerial meteoric diagenesis due to sea-level low stands (Guo et al., 2021; Luo et al., 2021, 2022) may infer more oxidizing environments at ca. 20–120 m and 440–500 m intervals of Well NK1. The Pr/Ph ratio records are consistent with the diagenetic facies in Well NK1 (Fig. 3E), showing higher ratio values indicative of more oxidizing environments (Didyk et al., 1978). Thus, the good positive correlation between contents of *n*-$C_{14–18}$ FAs and values of Pr/Ph (Fig. 4C) suggests that *n*-$C_{14–18}$ FAs are present in higher amounts under more oxygenated conditions. This occurrence, as mentioned above and explained below, should be due to the importance of terrestrial nutrient input for coral reef production, leading to higher abundances of *n*-$C_{14–18}$ FAs corresponding to more oxidizing conditions (and extensive meteoric diagenesis) during sea-level low stands. Nevertheless, it should also reflect that *n*-$C_{14–18}$ FAs in coral reef carbonates are highly resistant to oxic environments (and aerobic degradation).

The present study on *n*-$C_{14–18}$ FAs in Well NK1, together with previous studies on glycerol dialkyl glycerol tetraethers (GDGTs) in Well XK1 (Shao et al., 2017a, b) demonstrate the conservative behavior of lipid biomarkers in coral reef carbonates.

This suggests that lipid biomarkers are, to a large extent, protected by the initial coral skeletons from post-depositional diagenetic (i.e., recrystallization and dolomitization) and degradation alteration. This is further supported by the biomarker composition in Well NK1 coral reef carbonates that shows a high similarity to that in modern corals. For example, the majority of FAs that are dominated by short-chain *n*-FAs in Well NK1 coral reefs (Fig. 2A; Supplementary Fig. S2) is compatible with lipid studies on modern corals, showing the predominance of FAs (Treignier et al., 2008; Tolosa et al., 2011) that consist mainly of short-chain *n*-FAs (e.g., Imbs and Yakovleva, 2012; Kneeland et al., 2013; Radice et al., 2019; Rocker et al., 2019). Besides, the dominance of marine-sourced short-chain compound classes in Well NK1 (Figs. 2B–E; Supplementary Fig. S2) is consistent with the records of $\delta^{13}C$, C/N and $n\text{-}C_{25–27}/n\text{-}C_{15–17}$ in adjacent core 17962 which reveal that sedimentary OM is mainly of marine origin (Jia et al., 2002). This is followed by a recent study on nearby ODP Site 1143 (O'Brien et al., 2014) showing substantially low GDGTs-derived BIT values (mostly <0.2), which typically suggest a predominant contribution of marine OM input (Hopmans et al., 2004). These consistencies demonstrate the reliability of coral reef carbonate biomarkers that can preserve the initial environmental information.

4.3 Production of n-$C_{14–18}$ FAs in coral reefs linked to surface production since the Late Miocene

As discussed above, $n\text{-}C_{14–18}$ FAs are conservative in carbonate deposits, thereby allowing them to infer past changes in the production of Well NK1 coral reefs. The $n\text{-}C_{14–18}$ FAs inferred coral reef production exhibits a generally decreased trend during the Late Miocene–Pliocene (ca. 10.5–2.6 Ma) followed by a substantial increase with varying oscillations since the Pleistocene on million-year timescales (Fig. 5A), which

resembles largely to the Ln(Ba/Ti) ratio in Well NK1 (Fig. 5B). Biogenic Ba is considered as a good proxy for surface production in global oceans (Dymond et al., 1992; Francois et al., 1995), including the southern SCS (Zhang et al., 2009; Li et al., 2018). The Ln(Ba/Ti) ratio has been recently applied for Well XK1 coral reefs to reconstruct surface production in the northern SCS since the early Pliocene (Wu et al., 2019). Therefore, the large similarity between profiles of *n*-$C_{14–18}$ FAs and Ln(Ba/Ti) in Well NK1 (Figs. 5A–B) demonstrates that the production in coral reefs is closely linked to surface production. This is further supported by many other independent production records in adjacent ODP Site 1143, showing largely similar decreased trends in surface production since the Late Miocene on million-year timescales (Figs. 5C–F), such as opal (Li et al., 2002; Wang et al., 2004; Wan et al., 2006), Ba/Ti (Zhang et al., 2009), diatom (Lu et al., 2003) and radiolarian (Chen et al., 2003). However, records of Ba/Ti, diatom and radiolarian indicate that surface production shifted to rise after ca. 0.6 Ma (Figs. 5D–F; Yang et al., 2002; Lu et al., 2003; Zhang et al., 2009), much later than inferred from records of *n*-$C_{14–18}$ FAs and Ln(Ba/Ti) in Well NK1 (Figs. 5A–B; this study) and opal in ODP Site 1143 (Fig. 5C; Li et al., 2002; Wang et al., 2004; Wan et al., 2006). Besides, contents of *n*-$C_{14–18}$ FAs and values of Ln(Ba/Ti) in Well NK1 are peaked at ca. 0.5–0.7 and 1.2–1.4 Ma (Figs. 5A–B) likely reflective of extremely high production events in the Quaternary southern SCS; however, they are not found in the production records from ODP Site 1143 (Figs. 5C–F). These discrepancies could be attributed to the different sample resolutions among these studies and/or the different implications of these proxy records. For example, fossil diatoms and radiolarians are critically dependent on the production of diatoms and radiolarians in surface waters, respectively; whereas biogenic opal reflects the production of siliceous organisms, including diatoms and radiolarians (Wei et al.,

2003; Wan et al., 2006).

In summary, our *n*-$C_{14–18}$ FA records match well with many other independent paleo-production records in most parts of Well NK1 and ODP Site 1143 since the Late Miocene (Fig. 5), demonstrating the close coupling between coral reef production and surface phytoplankton production. This occurrence should be due to the common factor of nutrients in modulating production of endosymbiotic autotrophic coralline algae (i.e., dinoflagellats) and asymbiotic phytoplankton (i.e., diatoms) in the euphotic zone and/or the large dependence of heterotrophic corals on phytoplankton-governed food weds in surface waters. The *n*-$C_{14–18}$ FAs in Well NK1 coral reefs thus allows for a reevaluation of potential controlling factors, such as monsoon proposed previously, on long-term changes in surface production in the southern SCS since the Late Miocene on million-year timescales.

4.4 Potential factors controlling long-term production evolution in the southern SCS

Previous studies have revealed that surface phytoplankton production is critically limited by nutrient availability in surface waters in the oligotrophic oceans (Falkowski et al., 1998), including the southern SCS (Liu et al., 2002; Ning et al., 2004; Tang et al., 2004, 2006). The summertime upwelling-induced nutrients were proposed as the main nutrient resources delivered to offshore waters in the southern SCS, leading to higher nutrient loading in response to intensified summer monsoon in the early Late Miocene (i.e., 10–7 Ma; Chen et al., 2003; Lu et al., 2003; Wan et al., 2006). However, the proposed summer monsoon intensification is not compatible with many other proxy records from the monsoon-domain that indicate a major weakening of summer monsoon in the early Late Miocene (Guo et al., 2002; Jia et al., 2003; Sun and Wang, 2005; Clift et al., 2014; Gupta et al., 2015; Clift and Webb, 2019). For example,

planktonic foraminifer *Globigerina bulloides*, which is mainly produced at times of upwelling in summer, was nearly disappeared during ca. 11–7 Ma in the Arabian Sea upwelling regimes (Gupta et al., 2015).

Terrestrial nutrient influx from the Mekong River driven by chemical weathering was proposed as the complementary nutrient supply to the oligotrophic open southern SCS (Zhang et al., 2009). However, the inferred summer monsoon intensification that induced enhanced chemical weathering in the early Late Miocene (i.e., 10–7 Ma), as proposed by Zhang et al. (2009), was not supported by many other monsoon records (Guo et al., 2002; Jia et al., 2003; Sun and Wang, 2005; Clift et al., 2014; Gupta et al., 2015; Clift and Webb, 2019). This contradiction likely indicates that chemical weathering is not mainly governed by summer monsoon-induced precipitation, but is closely coupled to global temperature (Clift et al., 2014), thus leading to weakened chemical weathering since the Late Miocene (Zhang et al., 2009) as a response of global cooling (Fig. 6F; Zachos et al., 2001; Westerhold et al., 2020). However, this scenario did not occur in other sediment records. For example, a comprehensive study on clay mineralogy, major element, stable and radiogenic isotope abundances in the Bengal Fan indicates intense chemical weathering since the Late Miocene (i.e., ca. 7–1 Ma; Derry and France-Lanord, 1996). In contrast, other studies focused on the ^{10}Be records suggest long-term stability of global erosion and weathering rates through the late Cenozoic (Willenbring and von Blanckenburg, 2010; Lenard et al., 2020). In spite of these uncertainties, long-term changes of surface production in the southern SCS (Fig. 5) fail to follow any reconstructed context of chemical weathering variability since the Late Miocene shown above.

The strengthened wind regime resulting from global cooling has been invoked to interpret the rise in surface production in the Indian Ocean in the early Late Miocene

(Gupta et al., 2004). However, this is not so suitable for our study, as long-term evolution of paleo-production in the southern SCS does not track the progressive decrease in global temperature since the Late Miocene (Fig. 6F; Zachos et al., 2001; Westerhold et al., 2020). Besides, the reconstructed paleo-production in the southern SCS differs largely with the Pacific-Indian-Atlantic Oceans, where peaks in production occurred during ca. 6–4 Ma (Dickens and Owen, 1999; Hermoyian and Owen, 2001; Grant and Dickens, 2002). This appears to contradict the importance of global nutrient cycling in regulating regional production in the southern SCS since the Late Miocene.

In summary, the summer upwelling, chemical weathering, global cooling and oceanic nutrient cycling are difficult to interpret long-term changes of surface production in the southern SCS since the Late Miocene. This prompts us to consider the possible role of relative sea-level change, as we notice that *n*-$C_{14–18}$ FAs and Ln(Ba/Ti) change largely in parallel with terrigenous element Ti in Well NK1 (Figs. 6A–C) and respond almost inversely with sea-level variations since the Late Miocene (Figs. 6D–E; Shao et al., 2017a; Miller et al., 2020). Reduced sea levels in the early Late Miocene and since the Pleistocene (Figs. 6D–E; Shao et al., 2017a; Miller et al., 2020) are consistent with the subaerial meteoric diagenetic facies on Well NK1 coral reefs (Guo et al., 2021; Luo et al., 2021, 2022). During sea-level low stands, the emergence of the huge continental platforms led to the development of numerous drainage systems, and meanwhile, the study sites approached much closer to the river mouth, thus increasing terrestrial riverine input to offshore waters in the southern SCS (e.g., Jia et al., 2002; Hu et al., 2003; Pelejero, 2003; Wei et al., 2003; Huang and Tian, 2012). This is compatible with the global compilation suggesting that terrigenous sediment input into the oceans was largely regulated by sea-level variations since 5

Ma (Hay et al., 1988). Therefore, the elevated marine production documented in the southern SCS in the early Late Miocene and since the Pleistocene (Fig. 5) may be fertilized by higher terrigenous riverine nutrient input due to relatively low sea levels (Figs. 6D–E; Shao et al., 2017a; Miller et al., 2020). However, the meteoric diagenesis did not occur on Well NK1 coral reefs during ca. 2.6–1.5 Ma (Guo et al., 2021; Luo et al., 2021, 2022) featured by sea-level low stands (Figs. 6D–E; Shao et al., 2017a; Miller et al., 2020). This occurrence might be caused by the failure of regional sea-level decline to track tectonic subsidence, thus making the Meiji Atoll still submerged by the sea.

The proposed importance of relative sea-level change in controlling terrigenous riverine nutrient delivery to offshore waters appears to reconcile the argument of summer monsoon-induced upwelling-involved nutrients on interpreting long-term production variations in the southern SCS since the Late Miocene. This is supported by the covariation of higher terrestrial input and marine production in low-sea-level glacial times in cores 17962 (Jia et al., 2002; Hu et al., 2003) and MD05-2897 (Huang and Tian, 2012; Dong et al., 2019), but contradicts other observations showing higher production during high-sea-level interglacial periods (Jian et al., 2001; Wang and Abelmann, 2002; Wang and Li, 2003; Li et al., 2018). We believe these discrepancies may be reconciled by invoking most available proxy or seeking most reliable archive for reconstruction of paleo-production. As most of production recorders generated in surface waters would be altered to some extent during their descent in the water column and during burial in the sediment (e.g., Wei et al., 2003 and references therein), the production in shallow-water coral reefs should be more representative of surface production than inferred from seafloor sediments. This appears to signify a novel better approach to evaluate long-term paleo-production evolution in the euphotic zone

based on short-chain *n*-FAs in shallow-water coral reefs, which are widespread in tropical-subtropical oceans.

5. Conclusions

A series of lipid biomarkers are recovered from Well NK1 coral reef carbonates by an acid digestion extraction method and short-chain *n*-$C_{14–18}$ FAs are examined for their applicability to reconstruct paleo-production in coral reefs in the southern SCS since the Late Miocene. Comparisons with the isotopic ($\delta^{13}C$ and $\delta^{18}O$), mineral and redox (Pr/Ph) records demonstrate that *n*-$C_{14–18}$ *n*-FAs in coral reef carbonates are largely protected from or highly resistant to diagenetic and degradation alteration. The temporal distribution of short-chain *n*-FAs resembles largely to many other production records (i.e., Ln(Ba/Ti) and opal) since the Late Miocene, demonstrating that coral reef production is closely linked to surface water production in the southern SCS. This occurrence is attributable to the common factor of nutrients in modulating production of endosymbiotic coralline algae and asymbiotic phytoplankton and/or the large dependence of heterotrophic corals on primary production by asymbiotic phytoplankton in surface waters. Records of *n*-$C_{14–18}$ FAs and Ln(Ba/Ti) change almost in parallel with terrigenous element Ti in Well NK1 and largely reversed with relative sea-level variations since the Late Miocene, implying a long-term important role of sea-level change in terrestrial nutrient input and marine production in the southern SCS. This study highlights the feasibility of short-chain *n*-FAs as effective recorders for paleo-production in coral reefs that can be used to monitor surface water production in the geological past. We hope to develop the measurement on lipid biomarkers (i.e., compound-specific $\delta^{13}C$) to distinguish between autotrophic and heterotrophic production in coral reefs in future studies.

Declaration of competing interest

The authors declare that they have no known competing financial interests or personal relationships that could have appeared to influence the work reported in this paper.

Acknowledgements

The study is supported by the National Key R&D Program of China (2021YFC3100600), the Key Special Project for Introduced Talents Team of Southern Marine Science and Engineering Guangdong Laboratory (Guangzhou) (GML2019ZD0206), the Strategic Priority Research Program of the Chinese Academy of Sciences (XDA13010102), the National Natural Science Foundation of China (42176079, 41976063, 41976062 and 41676031) and K.C. Wong Education Foundation (GJTD-2018-13). Special thanks go to editors and two anonymous reviewers for their thoughtful and constructive comments that greatly improved the clarity and quality of the manuscript.

References

Anthony, K.R., Fabricius, K.E., 2000. Shifting roles of heterotrophy and autotrophy in coral energetics under varying turbidity. J. Exp. Mar. Biol. Ecol. 252, 221-253.

Blyth, A.J., Farrimond, P., Jones, M., 2006. An optimised method for the extraction and analysis of lipid biomarkers from stalagmites. Organic Geochemistry 37, 882-890.

Braga, J.C., Puga-Bernabéu, Á., Heindel, K., Patterson, M.A., Birgel, D., Peckmann, J., Sánchez-Almazo, I.M., Webster, J.M., Yokoyama, Y., Riding, R., 2019. Microbialites in Last glacial maximum and deglacial reefs of the Great Barrier

Reef (IODP Expedition 325, NE Australia). Palaeogeography, Palaeoclimatology, Palaeoecology 514, 1-17.

Chassot, E., Bonhommeau, S., Dulvy, N.K., Melin, F., Watson, R., Gascuel, D., Le Pape, O., 2010. Global marine primary production constrains fisheries catches. Ecol. Lett. 13, 495-505.

Chen, M.H., Wang, R.J., Yang, L.H., Han, J.X., Lu, J., 2003. Development of east Asian summer monsoon environments in the late Miocene: radiolarian evidence from Site 1143 of ODP Leg 184. Marine Geology 201, 163-177.

Clift, P.D., Wan, S.M., Blusztajn, J., 2014. Reconstructing chemical weathering, physical erosion and monsoon intensity since 25 Ma in the northern South China Sea: A review of competing proxies. Earth-Sci. Rev. 130, 86-102.

Clift, P.D., Webb, A.A.G., 2019. A history of the Asian monsoon and its interactions with solid Earth tectonics in Cenozoic South Asia. Geological Society, London, Special Publications 483, 631-652.

Dalsgaard, J., St John, M., Kattner, G., Muller-Navarra, D., Hagen, W., 2003. Fatty acid trophic markers in the pelagic marine environment, in: Southwards, A.J., Tyler, P.A., Young, C.M., Fuhrman, L.A. (Eds.), Advances in Marine Biology, Vol 46. Academic Press Ltd-Elsevier Science Ltd, London, pp. 225-340.

Derry, L.A., France-Lanord, C., 1996. Neogene Himalayan weathering history and river $^{87}Sr/^{86}Sr$: impact on the marine Sr record. Earth and Planetary Science Letters 142, 59-74.

Dickens, G.R., Owen, R.M., 1999. The latest Miocene–early Pliocene biogenic bloom: a revised Indian Ocean perspective. Marine Geology 161, 75-91

Didyk, B.M., Simoneit, B.R.T., Brassell, S.C., Eglinton, G., 1978. Organic geochemical indicators of palaeoenvironmental conditions of sedimentation.

Nature 272, 216-222.

Dong, L., Li, Z.Y., Jia, G.D., 2019. Archaeal ammonia oxidation plays a part in late Quaternary nitrogen cycling in the South China Sea. Earth and Planetary Science Letters 509, 38-46.

Dymond, J., Suess, E., Lyle, M., 1992. Barium in deep-sea sediment: A geochemical proxy for paleoproductivity. Paleoceanography 7, 163-181.

Grant, K.M., Dickens, G.R., 2002. Coupled productivity and carbon isotope records in the southwest Pacific Ocean during the late Miocene–early Pliocene biogenic bloom. Palaeogeography, Palaeoclimatology, Palaeoecology 187, 61-82.

Falkowski, P., 2012. Ocean Science: the power of plankton. Nature 483, S17-S20.

Falkowski, P.G., Barber, R.T., Smetacek, V., 1998. Biogeochemical controls and feedbacks on ocean primary production. science 281, 200-206.

Fang, G., Fang, W.-d., Fang, Y., Wang, K., 1998. A survey of studies on the South China Sea upper ocean circulation. Acta Oceanographica Taiwanica 37, 1-16.

Field, C.B., Behrenfeld, M.J., Randerson, J.T., Falkowski, P., 1998. Primary production of the biosphere: integrating terrestrial and oceanic components. science 281, 237-240.

Francois, R., Honjo, S., Manganini, S.J., Ravizza, G.E., 1995. Biogenic barium fluxes to the deep sea: Implications for paleoproductivity reconstruction. Global Biogeochemical Cycles 9, 289-303.

Gogou, A., Stephanou, E.G., 2004. Marine organic geochemistry of the Eastern Mediterranean: 2. Polar biomarkers in Cretan Sea surficial sediments. Marine Chemistry 85, 1-25.

Grottoli, A.G., Rodrigues, L.J., Palardy, J.E., 2006. Heterotrophic plasticity and resilience in bleached corals. Nature 440, 1186-1189.

Guo, W., Jia, G.D., Ye, F., Xiao, H.Y., Zhang, Z.Y., 2019. Lipid biomarkers in suspended particulate matter and surface sediments in the Pearl River Estuary, a subtropical estuary in southern China. Science of the Total Environment 646, 416-426.

Guo, Y., Deng, W., Liu, X., Kong, K., Yan, W., Wei, G., 2021. Clumped isotope geochemistry of island carbonates in the South China Sea: Implications for early diagenesis and dolomitization. Marine Geology 437.

Guo, Z.T., Ruddiman, W.F., Hao, Q.Z., Wu, H.B., Qiao, Y.S., Zhu, R.X., Peng, S.Z., Wei, J.J., Yuan, B.Y., Liu, T.S., 2002. Onset of Asian desertification by 22 Myr ago inferred from loess deposits in China. Nature 416, 159-163.

Gupta, A.K., Singh, R.K., Joseph, S., Thomas, E., 2004. Indian Ocean high-productivity event (10-8 Ma): Linked to global cooling or to the initiation of the Indian monsoons? Geology 32, 753-756.

Gupta, A.K., Yuvaraja, A., Prakasam, M., Clemens, S.C., Velu, A., 2015. Evolution of the South Asian monsoon wind system since the late Middle Miocene. Palaeogeography Palaeoclimatology Palaeoecology 438, 160-167.

Han, T., Yu, K.F., Yan, H.Q., Deng, W.F., Liu, Y., Xu, S.D., Tao, S.C., Zhang, H.L., Wang, S.P., 2019. Links between the coral $\delta^{13}C$ record of primary productivity variations in the northern South China Sea and the East Asian Winter Monsoon. Geophysical Research Letters 46, 14586-14594.

Hay, W.W., Sloan, J.L., Wold, C.N., 1988. Mass/age distribution and composition of sediments on the ocean floor and the global rate of sediment subduction. Journal of Geophysical Research: Solid Earth 93, 14933-14940.

He, J., Zhao, M., Wang, P., Li, L., Li, Q., 2013. Changes in phytoplankton productivity and community structure in the northern South China Sea during the past 260 ka.

Palaeogeography, Palaeoclimatology, Palaeoecology 392, 312-323.

Heindel, K., Birgel, D., Brunner, B., Thiel, V., Westphal, H., Gischler, E., Ziegenbalg, S.B., Cabioch, G., Sjövall, P., Peckmann, J., 2012. Post-glacial microbialite formation in coral reefs of the Pacific, Atlantic, and Indian Oceans. Chemical Geology 304, 117-130.

Heindel, K., Birgel, D., Peckmann, J.r., Kuhnert, H., Westphal, H., 2010. Formation of deglacial microbialites in coral reefs off Tahiti (IODP 310) involving sulfate-reducing bacteria. Palaios 25, 618-635.

Hermoyian, C.S., Owen, R.M., 2001. Late Miocene-early Pliocene biogenic bloom: Evidence from low-productivity regions of the Indian and Atlantic Oceans. Paleoceanography 16, 95-100.

Hernández-Sánchez, M.T., LaRowe, D.E., Deng, F.F., Homoky, W.B., Browning, T.J., Martin, P., Mills, R.A., Pancost, R.D., 2014. Further insights into how sediment redox status controls the preservation and composition of sedimentary biomarkers. Organic Geochemistry 76, 220-234.

Hoefs, M.J.L., Rijpstra, W.I.C., Sinninghe Damsté, J.S., 2002. The influence of oxic degradation on the sedimentary biomarker record I: Evidence from Madeira Abyssal Plain turbidites. Geochimica et Cosmochimica Acta 66, 2719-2735.

Hopmans, E.C., Weijers, J.W.H., Schefuss, E., Herfort, L., Sinninghe Damsté, J.S., Schouten, S., 2004. A novel proxy for terrestrial organic matter in sediments based on branched and isoprenoid tetraether lipids. Earth and Planetary Science Letters 224, 107-116.

Houlbrèque, F., Ferrier-Pagès, C., 2009. Heterotrophy in tropical scleractinian corals. Biological Reviews 84, 1-17.

Hu, J., Peng, P.a., Chivas, A.R., 2009. Molecular biomarker evidence of origins and

transport of organic matter in sediments of the Pearl River estuary and adjacent South China Sea. Applied Geochemistry 24, 1666-1676.

Hu, J.F., Peng, P., Fang, D.Y., Jia, G.D., Jian, Z.M., Wang, P.X., 2003. No aridity in Sunda Land during the Last Glaciation: Evidence from molecular-isotopic stratigraphy of long-chain *n*-alkanes. Palaeogeography Palaeoclimatology Palaeoecology 210, 269-281.

Huang, E., Tian, J., 2012. Sea-level rises at Heinrich stadials of early Marine Isotope Stage 3: Evidence of terrigenous *n*-alkane input in the southern South China Sea. Global and Planetary Change 94-95, 1-12.

Imbs, A., Yakovleva, I., 2012. Dynamics of lipid and fatty acid composition of shallow-water corals under thermal stress: an experimental approach. Coral Reefs 31, 41-53.

Jia, G.D., Peng, P.A., Fang, D.Y., 2002. Burial of different types of organic carbon in core 17962 from South China Sea since the last glacial period. Quaternary Research 58, 93-100.

Jia, G.D., Peng, P.A., Zhao, Q.H., Jian, Z.M., 2003. Changes in terrestrial ecosystem since 30 Ma in East Asia: Stable isotope evidence from black carbon in the South China Sea. Geology 31, 1093-1096.

Jian, Z., Huang, B., Kuhnt, W., Lin, H.L., 2001. Late quaternary upwelling intensity and east Asian monsoon forcing in the South China Sea. Quaternary Research 55, 363-370.

Kneeland, J., Hughen, K., Cervino, J., Hauff, B., Eglinton, T., 2013. Lipid biomarkers in *Symbiodinium* dinoflagellates: new indicators of thermal stress. Coral Reefs 32, 923-934.

Lenard, S.J., Lave, J., France-Lanord, C., Aumaitre, G., Bourlès, D.L., Keddadouche,

K., 2020. Steady erosion rates in the Himalayas through late Cenozoic climatic changes. Nature Geoscience 13, 448-452.

Li, G., Rashid, H., Zhong, L.F., Xu, X., Yan, W., Chen, Z., 2018. Changes in deep water oxygenation of the South China Sea since the last glacial period. Geophysical Research Letters 45, 9058-9066.

Li, G., Xu, W., Luo, Y., Liu, J., Zhao, J., Feng, Y., Cheng, J., Sun, Z., Xiang, R., Xu, M., Yan, W., 2018. Strontium isotope stratigraphy and LA-ICP-MS U-Pb carbonate age constraints on the Cenozoic tectonic evolution of the southern South China Sea. GSA Bulletin (accepted).

Li, J.R., Wang, R.J., Li, B.H., 2002. Variations of opal accumulation rates and paleoproductivity over the past 12 Ma at ODP Site 1143, southern South China Sea. Chinese Science Bulletin 47, 590-598.

Li, L., Li, Q., He, J., Wang, H., Ruan, Y., Li, J., 2015. Biomarker-derived phytoplankton community for summer monsoon reconstruction in the western South China Sea over the past 450 ka. Deep Sea Research Part II: Topical Studies in Oceanography 122, 118-130.

Liu, J., Ye, Z.Z., Han, G.R., Liu, X.B., Qu, G.S., 1997. Meteoric diagenesis in Pleistocene reef limestones of Xisha Islands, China. Journal of Asian Earth Sciences 15, 465-476.

Liu, K.K., Chao, S.Y., Shaw, P.T., Gong, G.C., Chen, C.C., Tang, T.Y., 2002. Monsoon-forced chlorophyll distribution and primary production in the South China Sea: observations and a numerical study. Deep-Sea Research Part I-Oceanographic Research Papers 49, 1387-1412.

Liu, N., Wang, Z.F., Li, X.S., Liu, L., Zhang, D.J., You, L., Luo, W., Liu, X.Y., 2019. Reef-carbonate diagenesis in the Pleistocene-Holocene of the well Xike#1, Xisha

Islands, South China Sea: implications on sea-level changes. Carbonates Evaporites 34, 1669-1687.

Lu, J., Chen, M., Wang, R., Vladimar, S.P., 2003. Late Miocene diatom records of ODP site 1143 in southern South China Sea. Journal of tropical oceanography 22, 1-7 (in Chinese).

Luo, Y., Li, G., Xu, W., Cheng, J., liu, J., Yan, W., 2022. Characteristics of Quaternary exposure surfaces in Well Nanke-1 and their relationship with sea-level changes. Journal of Tropical Oceanography, 41(1), 143-157 (in Chinese).

Luo, Y., Li, G., Xu, W., Liu, J., Cheng, J., Zhao, J., Yan, W., 2021. The effect of diagenesis on rare earth element geochemistry of the Quaternary carbonates at an isolated coral atoll in the South China Sea. Sedimentary Geology 420, 105933.

Miller, K.G., Browning, J.V., Schmelz, W.J., Kopp, R.E., Mountain, G.S., Wright, J.D., 2020. Cenozoic sea-level and cryospheric evolution from deep-sea geochemical and continental margin records. Sci. Adv. 6, eaaz1346.

Mudge, S.M., Norris, G.E., 1997. Lipid biomarkers in the Conwy Estuary (North Wales, UK): A comparison between fatty alcohols and sterols. Marine Chemistry 57, 61-84.

Ning, X., Chai, F., Xue, H., Cai, Y., Liu, C., Shi, J., 2004. Physical-biological oceanographic coupling influencing phytoplankton and primary production in the South China Sea. Journal of Geophysical Research-Oceans 109, C10005, doi:10010.11029/12004JC002365

O'Brien, C.L., Foster, G.L., Martinez-Boti, M.A., Abell, R., Rae, J.W.B., Pancost, R.D., 2014. High sea surface temperatures in tropical warm pools during the Pliocene. Nature Geoscience 7, 607-612.

Pelejero, C., 2003. Terrigenous *n*-alkane input in the South China Sea: high-resolution

records and surface sediments. Chemical Geology 200, 89-103.

Peters, K.E., Walters, C.C., Moldowan, J., 2005. The biomarker guide. Cambridge University Press.

Prahl, F.G., Dymond, J., Sparrow, M.A., 2000. Annual biomarker record for export production in the central Arabian Sea. Deep-Sea Research Part II-Topical Studies in Oceanography 47, 1581-1604.

Radice, V.Z., Brett, M.T., Fry, B., Fox, M.D., Hoegh-Guldberg, O., Dove, S.G., 2019. Evaluating coral trophic strategies using fatty acid composition and indices. PLoS One 14, 20.

Rocker, M.M., Francis, D.S., Fabricius, K.E., Willis, B.L., Bay, L.K., 2019. Temporal and spatial variation in fatty acid composition in Acropora tenuis corals along water quality gradients on the Great Barrier Reef, Australia. Coral Reefs 38, 215-228.

Shao, L., Cui, Y.C., Qiao, P.J., Zhang, D.J., Liu, X.Y., Zhang, C.L., 2017a. Sea-level changes and carbonate platform evolution of the Xisha Islands (South China Sea) since the Early Miocene. Palaeogeography Palaeoclimatology Palaeoecology 485, 504-516.

Shao, L., Li, Q.Y., Zhu, W.L., Zhang, D.J., Qiao, P.J., Liu, X.Y., You, L., Cui, Y.C., Dong, X.X., 2017b. Neogene carbonate platform development in the NW South China Sea: Litho-, bio- and chemo-stratigraphic evidence. Marine Geology 385, 233-243.

Sigman, D.M., Boyle, E.A., 2000. Glacial/interglacial variations in atmospheric carbon dioxide. Nature 407, 859-869.

Sinninghe Damsté, J.S., Rijpstra, W.I.C., Reichart, G.J., 2002. The influence of oxic degradation on the sedimentary biomarker record II. Evidence from Arabian Sea

sediments. Geochimica et Cosmochimica Acta 66, 2737-2754.

Strong, D., Flecker, R., Valdes, P.J., Wilkinson, I.P., Rees, J.G., Michaelides, K., Zong, Y.Q., Lloyd, J.M., Yu, F.L., Pancost, R.D., 2013. A new regional, mid-Holocene palaeoprecipitation signal of the Asian Summer Monsoon. Quaternary Science Reviews 78, 65-76.

Strong, D.J., Flecker, R., Valdes, P.J., Wilkinson, I.P., Rees, J.G., Zong, Y.Q., Lloyd, J.M., Garrett, E., Pancost, R.D., 2012. Organic matter distribution in the modern sediments of the Pearl River Estuary. Organic Geochemistry 49, 68-82.

Sun, X.J., Wang, P.X., 2005. How old is the Asian monsoon system? Palaeobotanical records from China. Palaeogeography Palaeoclimatology Palaeoecology 222, 181-222.

Tang, D.L., Kawamura, H., Shi, P., Takahashi, W., Guan, L., Shimada, T., Sakaida, F., Isoguchi, O., 2006. Seasonal phytoplankton blooms associated with monsoonal influences and coastal environments in the sea areas either side of the Indochina Peninsula. Journal of Geophysical Research-Biogeosciences 111, G01010.

Tang, D.L., Kawamura, H., Van Dien, T., Lee, M., 2004. Offshore phytoplankton biomass increase and its oceanographic causes in the South China Sea. Mar. Ecol.-Prog. Ser. 268, 31-41.

Tolosa, I., Treignier, C., Grover, R., Ferrier-Pages, C., 2011. Impact of feeding and short-term temperature stress on the content and isotopic signature of fatty acids, sterols, and alcohols in the scleractinian coral Turbinaria reniformis. Coral Reefs 30, 763-774.

Treignier, C., Derenne, S., Saliot, A., 2006. Terrestrial and marine *n*-alcohol inputs and degradation processes relating to a sudden turbidity current in the Zaire canyon. Organic Geochemistry 37, 1170-1184.

Treignier, C., Grover, R., Ferrier-Pages, C., Tolosa, I., 2008. Effect of light and feeding on the fatty acid and sterol composition of zooxanthellae and host tissue isolated from the scleractinian coral Turbinaria reniformis. Limnology and Oceanography 53, 2702-2710.

Versteegh, G.J.M., Zonneveld, K.A.F., de Lange, G.J., 2010. Selective aerobic and anaerobic degradation of lipids and palynomorphs in the Eastern Mediterranean since the onset of sapropel S1 deposition. Marine Geology 278, 177-192.

Volkman, J.K., 2006. Lipid markers for marine organic matter. Marine Organic Mattter: Biomarkers, Isotopes and DNA 2, 27-70.

Wakeham, S.G., Peterson, M.L., Hedges, J.I., Lee, C., 2002. Lipid biomarker fluxes in the Arabian Sea, with a comparison to the equatorial Pacific Ocean. Deep-Sea Research Part II-Topical Studies in Oceanography 49, 2265-2301.

Wan, S.M., Li, A.C., Clift, P.D., Jiang, H.Y., 2006. Development of the East Asian summer monsoon: Evidence from the sediment record in the South China Sea since 8.5 Ma. Palaeogeography Palaeoclimatology Palaeoecology 241, 139-159.

Wang, C.F., Zhang, H.B., Huang, X.Y., Huang, J.H., Xie, S.C., 2012. Optimization of acid digestion conditions on the extraction of fatty acids from stalagmites. Front. Earth Sci. 6, 109-114.

Wang, R., Abelmann, A., 2002. Radiolarian responses to paleoceanographic events of the southern South China Sea during the Pleistocene. Marine Micropaleontology 46, 25-44.

Wang, R., Li, J., Li, B., 2004. Data report: Late Miocene–Quaternary biogenic opal accumulation at ODP Site 1143, southern South China Sea, Proc. ODP, Sci. Results.

Wang, R.J., Li, J., 2003. Quaternary high-resolution opal record and its

paleoproductivity implication at ODP Site 1143, Southern South China Sea. Chinese Science Bulletin 48, 363-367.

Wang, Z.F., Huang, K.K., Zhang, D.J., You, L., Liu, X.Y., Luo, W., 2018. Maturation of Neogene dolomite from Xuande Atoll of Xisha archipelago, the South China Sea. Marine and Petroleum Geology 92, 51-64.

Wei, G., Liu, Y., Li, X., Chen, M., Wei, W., 2003. High-resolution elemental records from the South China Sea and their paleoproductivity implications. Paleoceanography 18, 1054.

Westerhold, T., Marwan, N., Drury, A.J., Liebrand, D., Agnini, C., Anagnostou, E., Barnet, J.S.K., Bohaty, S.M., De Vleeschouwer, D., Florindo, F., Frederichs, T., Hodell, D.A., Holbourn, A.E., Kroon, D., Lauretano, V., Littler, K., Lourens, L.J., Lyle, M., Palike, H., Rohl, U., Tian, J., Wilkens, R.H., Wilson, P.A., Zachos, J.C., 2020. An astronomically dated record of Earth's climate and its predictability over the last 66 million years. Science 369, 1383-1387.

Willenbring, J.K., Von Blanckenburg, F., 2010. Long-term stability of global erosion rates and weathering during late-Cenozoic cooling. Nature 465, 211-214.

Wood, R., 1993. Nutrients, predation and the history of reef-building. Palaios, 526-543.

Wood, R., 1995. The changing biology of reef-building. Palaios, 517-529

Wu, F., Xie, X.N., Betzler, C., Zhu, W.L., Zhu, Y.H., Guo, L.Y., Ma, Z.L., Bai, H.Q., Ma, B.J., 2019. The impact of eustatic sea-level fluctuations, temperature variations and nutrient-level changes since the Pliocene on tropical carbonate platform (Xisha Islands, South China Sea). Palaeogeography Palaeoclimatology Palaeoecology 514, 373-385.

Xu, S.D., Yu, K.F., Zhang, Z.N., Chen, B.A., Qin, Z.J., Huang, X.Y., Jiang, W., Wang, Y.X., Wang, Y.H., 2020. Intergeneric differences in trophic status of Scleractinian

Corals from Weizhou Island, northern South China Sea: Implication for their different environmental stress tolerance. Journal of Geophysical Research-Biogeosciences 124, e2019JG005451.

Yang, L.H., Chen, M.H., Wang, R.J., Zhen, F., 2002. Radiolarian record to paleoecological environment change events over the past 1.2 MaBP in the southern South China Sea. Chinese Science Bulletin 47, 1478-1483.

Yi, L., Deng, C., Yan, W., Wu, H., Zhang, C., Xu, W., Su, X., He, H., Guo, Z., 2021. Neogene–quaternary magnetostratigraphy of the biogenic reef sequence of core NK–1 in Nansha Qundao, South China Sea. Science Bulletin 66, 200-203.

Yu, K.F., 2012. Coral reefs in the South China Sea: their response to and records on past environmental changes. Science China-Earth Sciences 55, 1217-1229.

Zachos, J., Pagani, M., Sloan, L., Thomas, E., Billups, K., 2001. Trends, rhythms, and aberrations in global climate 65 Ma to present. Science 292, 686-693.

Zhang, H., Liu, C., Jin, X., Shi, J., Zhao, S., Jian, Z., 2016. Dynamics of primary productivity in the northern South China Sea over the past 24,000 years. Geochemistry Geophysics Geosystems 17, 4878-4891.

Zhang, L.L., Chen, M.H., Xiang, R., Zhang, L.L., Lu, J., 2009. Productivity and continental denudation history from the South China Sea since the late Miocene. Marine Micropaleontology 72, 76-85.

Zhao, M.X., Yu, K.F., Shi, Q., Chen, T.R., Zhang, H.L., Chen, T.G., 2013. Coral communities of the remote atoll reefs in the Nansha Islands, southern South China Sea. Environmental Monitoring and Assessment 185, 7381-7392.

Zhao, M.X., Zhang, H.Y., Zhong, Y., Xu, X.F., Yan, H.Q., Li, G., Yan, W., 2021. Microstructural characteristics of the stony coral genus Acropora useful to coral reef paleoecology and modern conservation. Ecol. Evol. 11, 3093-3109.

Zhu, X., Jia, G., Mao, S., Sun, Y., Wu, N., Tian, Y., Xu, W., Yan, W., 2020. Long chain 1,14-diols as potential indicators for upper water stratification in the open South China Sea. Ecological Indicators 110, 105900.

Zhu, X., Mao, S., Wu, N., Sun, Y., Guan, H., 2014. Molecular and stable carbon isotopic compositions of saturated fatty acids within one sedimentary profile in the Shenhu, northern South China Sea: Source implications. Journal of Asian Earth Sciences 92, 262-275.

Zhu, X., Jia, G., Tian, Y., Mo, A., Xu, W., Miao, L., Xu, S., Yan, W., 2021. Photosynthetic production determines bottom water oxygen variations in the upwelling coastal South China Sea over recent decades. Frontiers in Earth Science 9, 759317.

Lists of Figures

Fig. 1 Location of coral reefs (red; A) and sediment cores (yellow; B) mentioned in this study. (A): NK1 (this study) on the Meiji Atoll in the Nansha Islands in the southern SCS, and XC1 (Liu et al., 1997), XK1 (Shao et al., 2017a, b; Liu et al., 2019; Wu et al., 2019) and ZK1 (Wang et al., 2018) on the Xisha Islands in the northern SCS. (B): sediment cores 17954 (Jian et al., 2001), 17957 (Wang and Abelmann, 2002), 17961&17964 (Pelejero, 2003), 17962 (Jia et al., 2002; Hu et al., 2003), MD05-2901 (Li et al., 2015), MD05-2897 (Huang and Tian, 2012; Dong et al., 2019), NS93-5 (Wei et al., 2003), B9 (Li et al., 2018), and ODP Site 1143 (Li et al., 2002; Yang et al., 2002; Chen et al., 2003; Lu et al., 2003; Wang and Li, 2003; Wang et al., 2004; Wan et al., 2006; Zhang et al., 2009; O'Brien et al., 2014) around the study area. Surface currents in winter (black dotted lines) and summer (red solid lines) in Fig. 1B are redrawn from Fang et al. (1998). The Vietnam Upwelling in summer is marked with a grey box in Fig. 1B (Liu et al., 2002; Tang et al., 2004, 2006).

Fig. 2 Average abundances (μg/g) of total *n*-FAs, *un*-FAs (unsaturated FAs), *br*-FAs and *n*-OLs (*n*-alcohols) (A), and fractional abundances (%) of individual compounds in each class: *n*-FA (B), *un*-FA (C), *br*-FA (D) and *n*-OL (E). Error bars indicate the standard deviations. Numbers denote carbon numbers. In the *un*-FA fraction, *n*-$C_{16:1}$: the sum of *n*-$C_{16:1\omega9}$ and *n*-$C_{16:1\omega7}$, *n*-$C_{18:1}$: the sum of *n*-$C_{18:1\omega9}$ and *n*-$C_{18:1\omega7}$, *n*-$C_{20:1}$: the sum of *n*-$C_{20:1\omega9}$ and *n*-$C_{20:1\omega7}$, *n*-$C_{22:1}$: the sum of *n*-$C_{22:1\omega9}$ and *n*-$C_{22:1\omega7}$.

Fig. 3 Depth profiles of *n*-$C_{14–18}$ FAs (A) and the Pr/Ph ratio (E) (this study), and isotopes (B–C) and minerals (D) (Guo et al., 2021; Luo et al., 2021, 2022) in Well NK1. In Fig. 3D, Ara, HMC, LMC and Dol indicate aragonite, high-Mg calcite, low-Mg calcite and dolomite, respectively. Grey columns denote two intervals at ca. 20–120 m and 440–500 m, which have experienced meteoric diagenesis under subaerial oxidizing conditions due to sea-level low stands (Guo et al., 2021; Luo et al., 2021, 2022)

Fig. 4 Linear correlations of contents of *n*-$C_{14–18}$ FAs with values of $\delta^{13}C$ (A), $\delta^{18}O$ (B) and Pr/Ph (C) in Well NK1.

Fig. 5 Temporal changes in *n*-$C_{14–18}$ FAs (A) and Ln(Ba/Ti) (B) in Well NK1 (this study), and opal (C) (Li et al., 2002; Wang et al., 2004; Wan et al., 2006) and Ba/Ti (D) (Zhang et al., 2009) in ODP Site 1143. The *n*-$C_{14–18}$ FA, Ln(Ba/Ti) and opal curves are smoothed by 3-point running average. Also shown are the depth profiles of diatoms (E) (Lu et al., 2003) and radiolarians (F) (Chen et al., 2003) with ages labeled in the curves based on age models in Wang et al. (2004).

Fig. 6 Comparisons of *n*-$C_{14–18}$ FAs (A), Ln(Ba/Ti) (B) and terrigenous element Ti (C) in Well NK1 (this study) with the global compilation of sea-level variations (D) (Miller et al., 2020), BIT records (E) (with lower values indicating higher sea levels) in Well XK1 in the northern SCS (Shao et al., 2017a) and global deep-sea $\delta^{18}O$ records (F) (Westerhold et al., 2020). The *n*-$C_{14–18}$ FA, Ln(Ba/Ti) and Ti curves are smoothed by 3-point running average. Grey columns are the same as in Fig. 3, denoting two intervals marked with meteoric diagenesis due to sea-level low stands (Guo et al., 2021; Luo et al., 2021, 2022). Yellow columns indicate two time-intervals with reduced sea levels, but are characterized by the disappearance of meteoric diagenesis on coral reef carbonates.

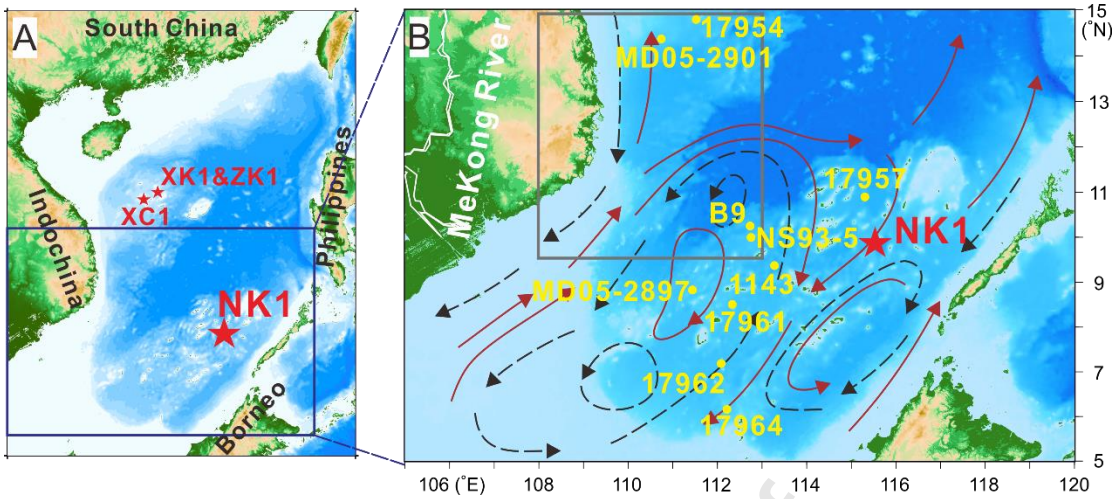

Fig. 1

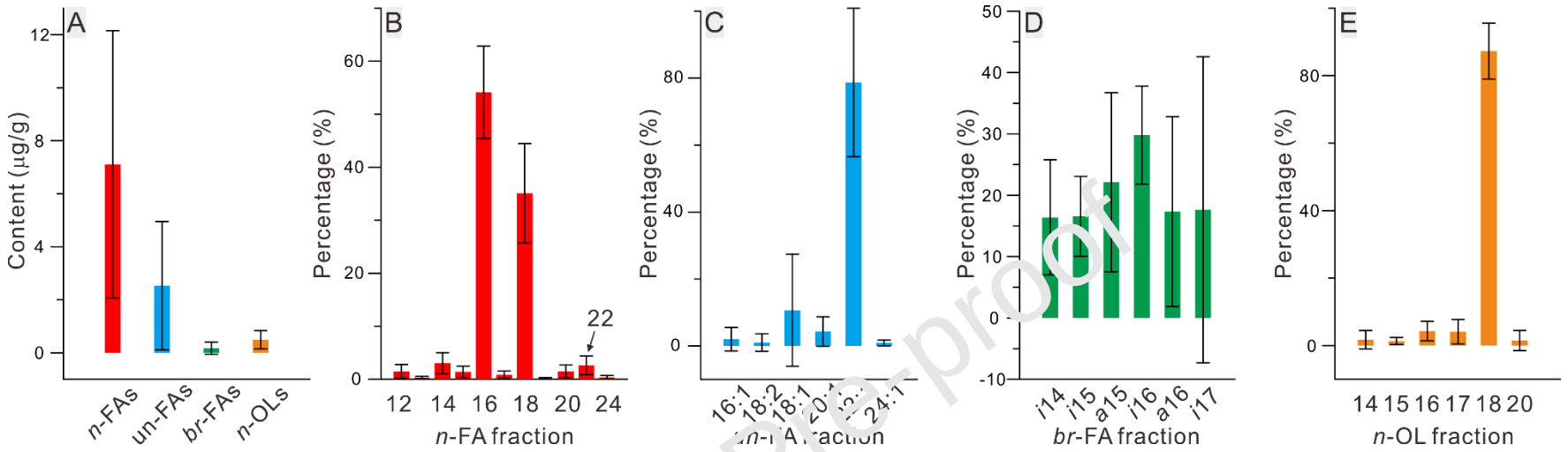

Fig. 2

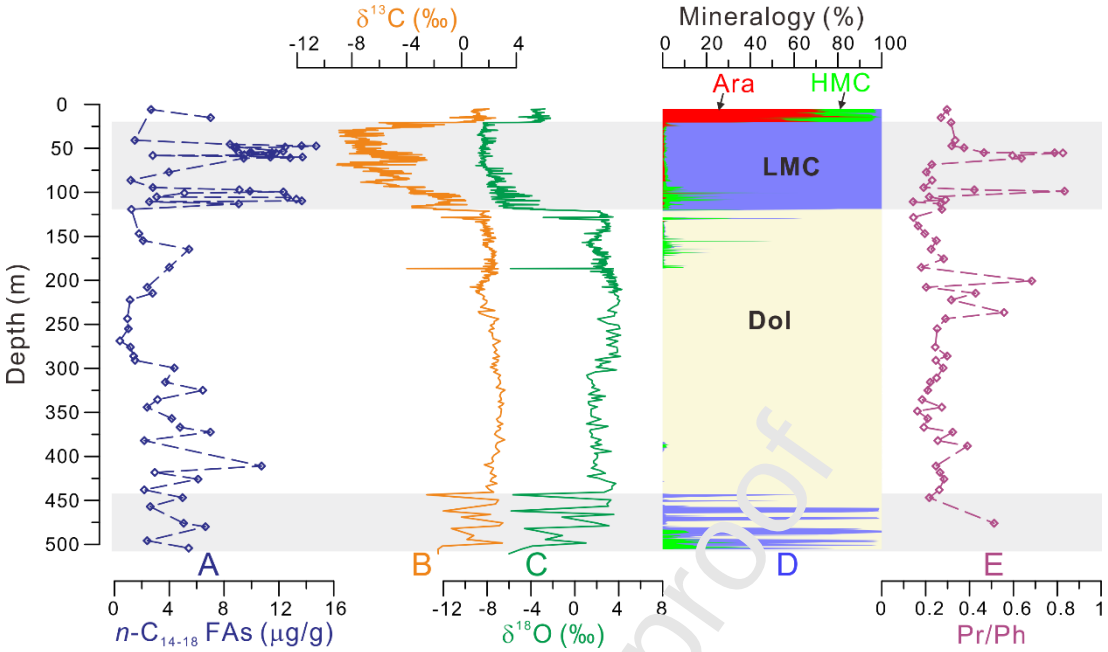

Fig. 3

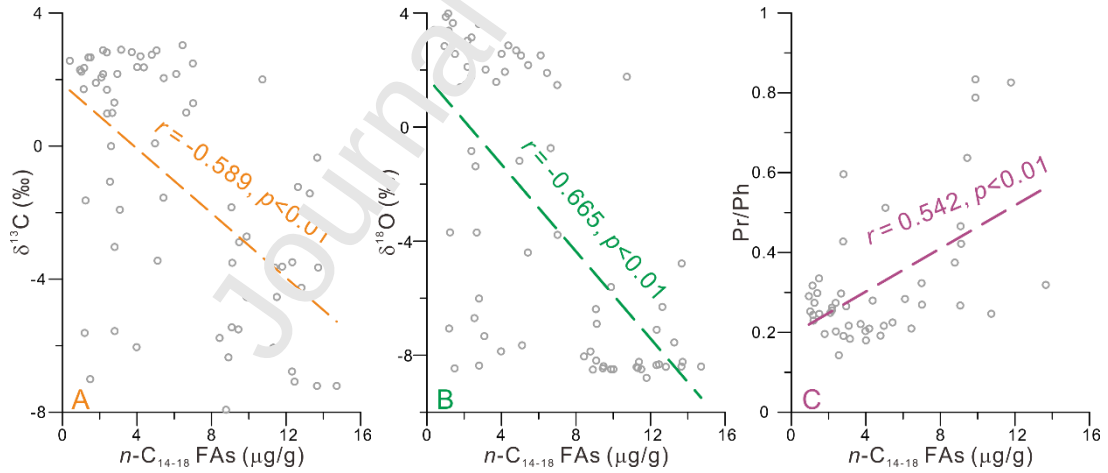

Fig. 4

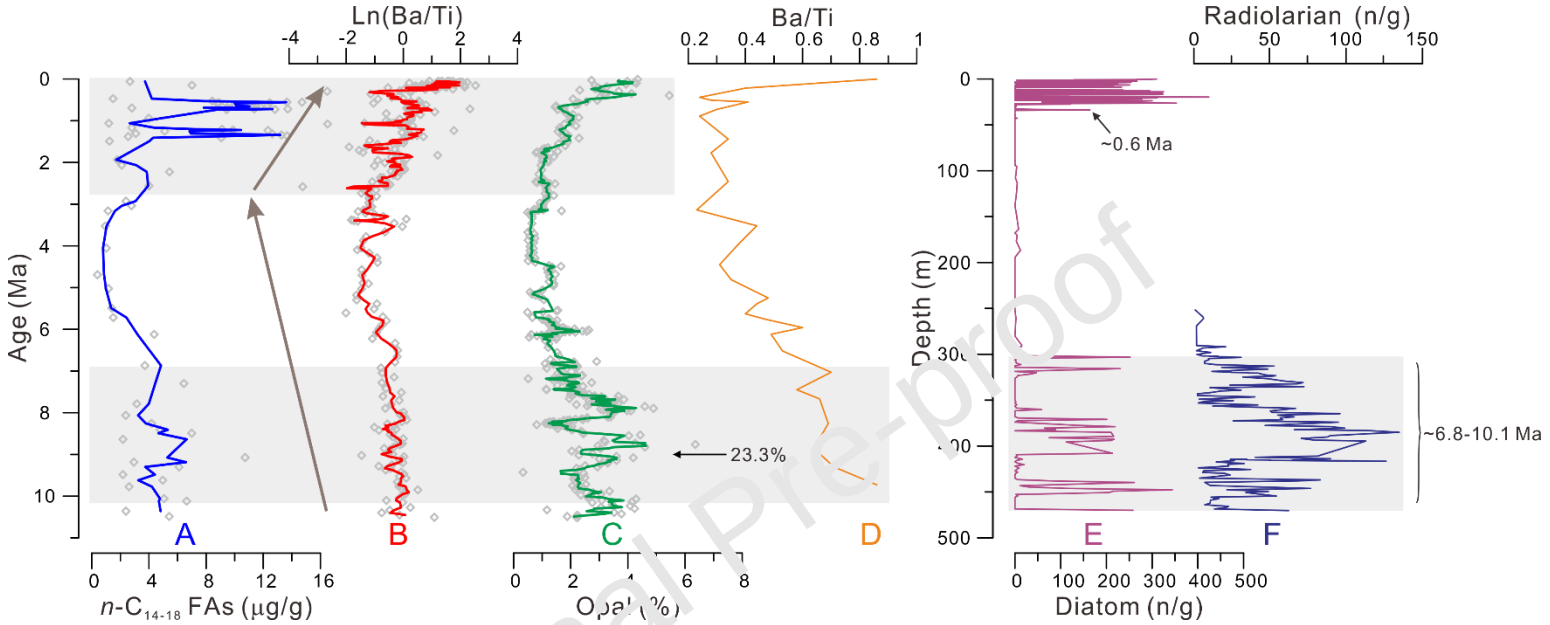

Fig. 5

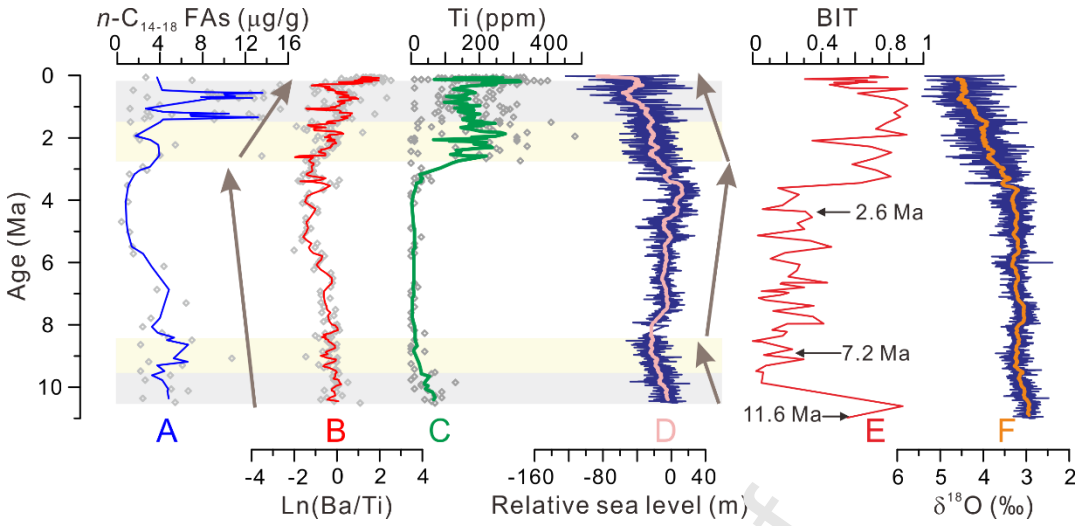

Fig. 6

Declaration of interests

√The authors declare that they have no known competing financial interests or personal relationships that could have appeared to influence the work reported in this paper.

☐The authors declare the following financial interests/personal relationships which may be considered as potential competing interests:

- ✓ A long coral reef well (NK1) in the southern SCS was studied
- ✓ OM-poor coral reef carbonates were decalcified and extracted for biomarkers
- ✓ Short-chain *n*-FAs reflect paleo-productivity in coral reefs since the Late Miocene
- ✓ Long-term productivity was governed by terrestrial nutrient related to sea level